RGMa inhibition promotes axonal growth and recovery after spinal cord injury

Katsuhiko Hata,[1] Masashi Fujitani,[1] Yuichi Yasuda,[2] Hideo Doya,[1] Tomoko Saito,[1] Satoru Yamagishi,[1] Bernhard K. Mueller,[3] and Toshihide Yamashita[1]

[1]Department of Neurobiology, Graduate School of Medicine, Chiba University, Chuo-ku, Chiba 260-8670, Japan
[2]Central Research Laboratories, Sysmex Corporation, Nishi-ku, Kobe 651-22, Japan
[3]Central Nervous System Research, Abbott GmbH and Company KG, 67061 Ludwigshafen, Germany

Repulsive guidance molecule (RGM) is a protein implicated in both axonal guidance and neural tube closure. We report RGMa as a potent inhibitor of axon regeneration in the adult central nervous system (CNS). RGMa inhibits mammalian CNS neurite outgrowth by a mechanism dependent on the activation of the RhoA–Rho kinase pathway. RGMa expression is observed in oligodendrocytes, myelinated fibers, and neurons of the adult rat spinal cord and is induced around the injury site after spinal cord injury. We developed an antibody to RGMa that efficiently blocks the effect of RGMa in vitro. Intrathecal administration of the antibody to rats with thoracic spinal cord hemisection results in significant axonal growth of the corticospinal tract and improves functional recovery. Thus, RGMa plays an important role in limiting axonal regeneration after CNS injury and the RGMa antibody offers a possible therapeutic agent in clinical conditions characterized by a failure of CNS regeneration.

Introduction

Axons of the central nervous system (CNS) demonstrate no functionally significant regeneration after injury, in contrast to those of the peripheral nervous system, which regenerate vigorously, leading often to complete functional recovery. This lack of regeneration generally results in partial disability or complete paralysis after a CNS injury. However, some adult CNS axons can grow through a peripheral nerve graft (David and Aguayo, 1981), suggesting that the local glial environment of the adult CNS is a major cause of the lack of regeneration. So far, three major inhibitors—Nogo, myelin-associated glycoprotein (MAG), and oligodendrocyte-myelin glycoprotein (OMgp)—expressed by oligodendrocytes and myelinated fiber tracts have been identified. Interestingly, all these inhibitors were found to bind to the Nogo receptor (NgR) in complex with p75 or TROY, members of the TNF receptor family, suggesting that they have common signaling pathways (Teng and Tang, 2005).

Correspondence to Toshihide Yamashita: t-yamashita@faculty.chiba-u.jp

Abbreviations used in this article: BBB, Basso-Beattie-Bresnahan locomotor rating scale; BDA, biotin-dextran amine; CNS, central nervous system; CSPG, chondroitin sulfate proteoglycan; CST, corticospinal tract; GFAP, glial fibrillary acidic protein; IB4, isolectin B4; MAG, myelin-associated glycoprotein; MOSP, myelin/oligodendrocyte-specific protein; NgR, Nogo receptor; OMgp, oligodendrocyte-myelin glycoprotein; PI-PLC, phosphatidylinositol-specific PLC; PLL, poly-L-lysine; RGM, repulsive guidance molecule; SCI, spinal cord injury; Tuj1, neuron-specific β tubulin III protein.

The online version of this article contains supplemental material.

However, some reports suggest that inhibition of these molecules alone is insufficient for regeneration after CNS injury (Teng and Tang, 2005). MAG knockout mice exhibited little or no enhancement of axonal regeneration in the spinal cord. There seems to be some controversy concerning Nogo knockout mice and NgR-deficient mice. Neither depletion of functional p75 nor administration of a soluble p75-Fc at the lesion site promoted regeneration of the injured spinal cord. These findings prompted us to search for new inhibitors.

Repulsive guidance molecule (RGM), which has been reported as the 33-kD mass tectum repellent in chick, induces the collapse of temporal but not nasal growth cones and guides temporal retinal axons in vitro (Stahl et al. 1990; Muller et al., 1996; Monnier et al., 2002). RGM binds to neogenin, identified as a netrin-1 receptor and homologue of DCC (deleted in colorectal cancer), mediating its repulsive activity toward retinal axons (Rajagopalan et al., 2004). During chick development, neogenin functions as a dependence receptor, inducing cell death in the absence of RGM (Matsunaga et al., 2004). Three mouse proteins, homologous to chick RGM, termed mRGMa, -b, and -c (Niederkofler et al., 2004; Oldekamp et al., 2004; Schmidtmer and Engelkamp, 2004) have been reported. Mouse RGMa is highly homologous (80% identity) to chick RGM. Functional studies in RGMa mutant mice revealed the role of RGMa in controlling cephalic neural tube closure (Niederkofler et al., 2004).

The Journal of Cell Biology, Vol. 173, No. 1, April 10, 2006 47–58
http://www.jcb.org/cgi/doi/10.1083/jcb.200508143

We reported that up-regulation of RGMa was observed at the lesioned or damaged site after spinal cord injury (SCI) in rats (Schwab et al., 2005a) and focal cerebral ischemia and traumatic brain injury in humans (Schwab et al., 2005b). In addition, neogenin and other netrin-1 receptors are constitutively expressed by neurons and glial cells in the adult rat spinal cord (Manitt et al., 2004). These findings prompted us to hypothesize that RGMa may play a role in inhibiting axonal regeneration after CNS injury. In this study, we show that RGMa inhibits neurite outgrowth in postnatal cerebellar neurons in vitro. RGMa expression is induced after SCI in rats at the lesion site, in the developing scar tissue, and on the myelinated fiber tracts. Local administration of a neutralizing antibody to RGMa significantly facilitates locomotor improvement and axon regeneration after SCI.

Results

RGMa inhibits neurite outgrowth by a mechanism dependent on the activation of the RhoA–Rho kinase pathway

We first asked whether RGM contributes to the inhibition of mammalian CNS neurite outgrowth in vitro. Cerebellar granule neurons were used because they express the receptor for RGMa (Fig. S1, available at http://www.jcb.org/cgi/content/full/jcb.200508143/DC1). We cultured cerebellar granule neurons from postnatal rats (postnatal days 7–9) on confluent monolayers of either CHO cells expressing rat RGMa (RGMa-CHO cells) or control CHO cells for 24 h and assessed the neurite outgrowth rate (the coculture assay). Neurite outgrowth was

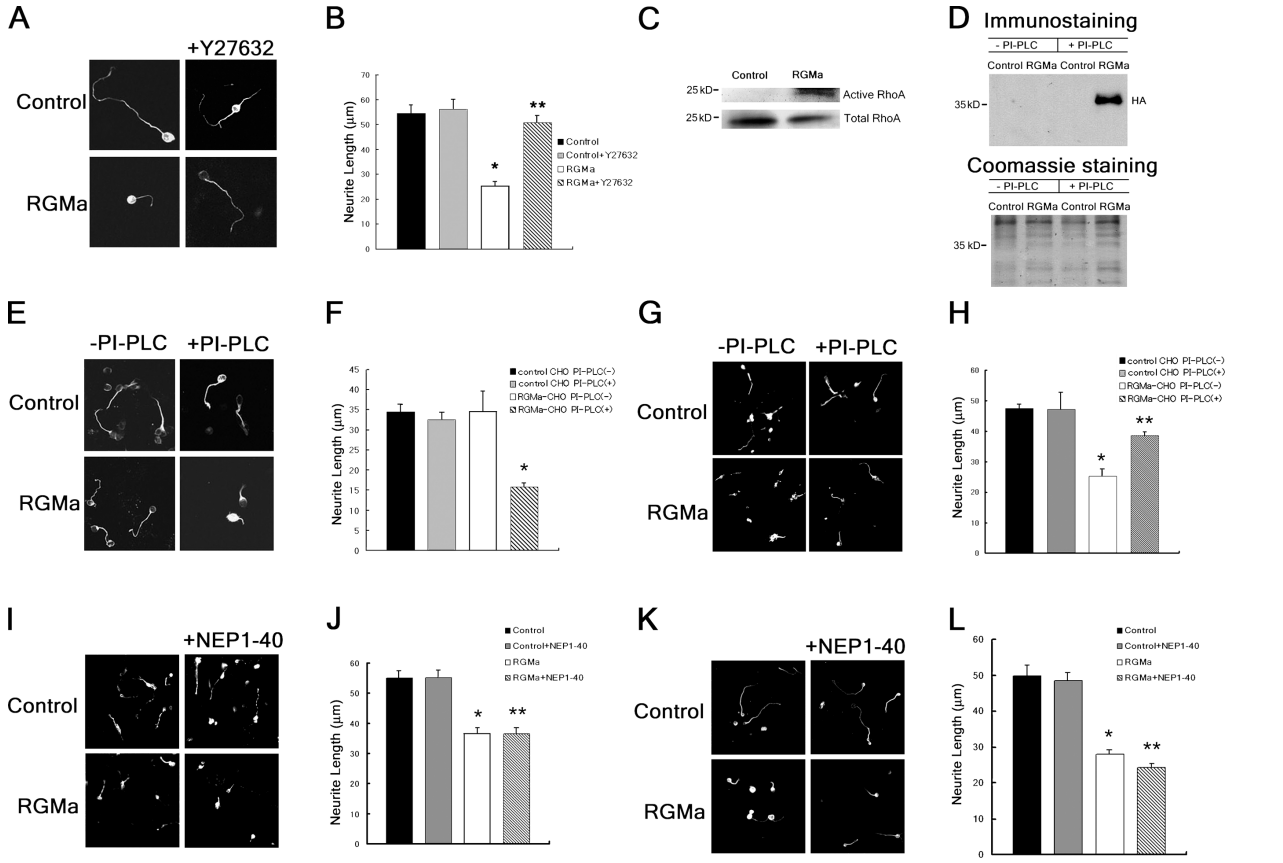

Figure 1. **Effects of membrane bound/diffusible RGMa on neurons.** (A) The membrane bound form of RGMa inhibits neurite outgrowth by a Rho-kinase–dependent mechanism. The cerebellar neurons were cultured for 24 h on control CHO cells (control) or RGMa-CHO cells (RGMa) in the presence or absence of 10 μM Y27632. (B) Mean length of the longest neurite per neuron. *, $P < 0.01$ compared with the control; **, $P < 0.01$ compared with RGMa (*t* test). (C) RGMa activates RhoA. The cerebellar neurons were treated for 10 min with conditioned media, derived from PI-PLC treatment of control CHO or RGMa-CHO cells. The active fraction of RhoA along with total RhoA was detected by Western blot. (D) Immunostaining of the supernatant from control/RGMa CHO cells treated with or without PI-PLC. The protein was detected by an anti-HA antibody. Coomassie staining was performed for the same samples. (E) The soluble form of RGMa inhibits neurite outgrowth. Neurons were cultured on PLL-coated chamber slides for 12 h in the conditioned media from untreated control CHO cells, PI-PLC–treated control CHO cells, untreated RGMa-CHO cells, or PI-PLC–treated RGMa-CHO cells. (F) Mean length of the longest neurite per neuron. *, $P < 0.01$ compared with the control CHO PI-PLC(+) (*t* test). (G) PI-PLC treatment reverses the inhibitory effect of RGMa-CHO cells. Neurons were cultured for 24 h on control/RGMa CHO cells pretreated with or without PI-PLC. (H) Mean length of the longest neurite per neuron. *, $P < 0.01$ compared with the control CHO PI-PLC(−); **, $P < 0.01$ compared with RGMa-CHO PI-PLC(−) (*t* test). There is no significant difference between the control CHO PI-PLC(+) and RGMa-CHO PI-PLC(+). (I–L) RGMa inhibits neurite outgrowth by an NgR-independent mechanism. (I) The cerebellar neurons were cultured for 24 h on control/RGMa CHO cells in the presence or absence of 1 μM NEP1-40. (J) Mean length of the longest neurite per neuron. *, $P < 0.01$ compared with the control; **, $P < 0.01$ compared with the control + NEP1-40 (*t* test). There is no significant difference between RGMa and RGMa+NEP1-40. (K) The neurons were cultured on PLL-coated chamber slides for 24 h in the conditioned media from PI-PLC–treated control/RGMa CHO cells in the presence or absence of 1 μM NEP1-40. (L) Mean length of the longest neurite per neuron. *, $P < 0.01$ compared with the control; **, $P < 0.01$ compared with the control + NEP1-40 (*t* test). There is no significant difference between RGMa and RGMa + NEP1-40. Data are represented as the mean ± SEM of three independent experiments.

significantly inhibited when grown on RGMa-CHO cells (Fig. 1, A and B). To explore the signal transduction mechanism involved in the inhibition of neurite outgrowth, we assessed whether the neuronal effects of RGMa are dependent on the small GTPase RhoA or its downstream effector, the Rho-associated serine/threonine kinase (Rho kinase). We cultured the neurons on RGMa-CHO cells in the presence of 10 μM Y27632, a specific inhibitor of Rho kinase (Uehata et al., 1997), for 24 h and observed that the inhibitory activity of RGMa was abolished by Y27632 (Fig. 1, A and B). To directly assess whether RhoA is involved in the signal transduction of RGMa, the activity of RhoA was determined using the RhoA binding domain of the effector protein, Rhotekin (Ren et al., 1999; Fig. 1 C). The assay revealed that within 10 min after the addition of soluble RGMa (see the following paragraph), extracts of the cells contained increased amounts of GTP-RhoA compared with those of the control cells. These results suggest that RGMa inhibits neurite outgrowth by a mechanism dependent on the activation of the RhoA–Rho kinase pathway.

Because rat RGMa, as well as chick RGM (Monnier et al., 2002), may be a glycosylphosphatidylinositol-linked protein that anchors to the cell surface, we examined whether the soluble form of RGMa shows the same activity. The RGMa-CHO or control CHO cells were treated with phosphatidylinositol-specific PLC (PI-PLC). RGMa was released into the supernatant from the RGMa-CHO cells by the treatment as assessed by immunodetection on Western blots (Fig. 1 D). We then cultured the neurons with the supernatant for 12 h and measured the neurite length (Fig. 1, E and F; the soluble RGMa assay). There was no significant difference in the neurite length between neurons cultured in conditioned media from PI-PLC–treated control CHO cells and those treated with media from nontreated control CHO cells, demonstrating that PI-PLC itself had no effect on neurite outgrowth. Neurite outgrowth was significantly inhibited when the neurons were cultured in conditioned media from PI-PLC–treated RGMa-CHO cells, demonstrating that the soluble form of RGMa inhibited neurite outgrowth. Next, we cultured the neurons on PI-PLC–treated RGMa-CHO cells for 24 h and observed that the inhibitory activity of RGMa was significantly reduced (Fig. 1, G and H), suggesting that RGMa was released from the cells by the PI-PLC treatment.

The findings that RGMa activates RhoA and inhibits neurite outgrowth prompted us to examine whether RGMa signals via the NgR. To determine whether RGMa binds to the NgR, the neurons were cultured for 24 h on RGMa-CHO cells (Fig. 1, I and J) or with soluble RGMa (Fig. 1, K and L) in the presence or absence of 1 μM NEP1-40 (GrandPre et al., 2002). The inhibitory effect of RGMa was not significantly altered by NEP1-40, suggesting that RGMa inhibits neurite outgrowth by an NgR-independent mechanism.

RGMa protein is expressed in purified CNS myelin and adult rat spinal cord

To examine the protein expression of RGMa in the adult CNS, antisera were generated against a synthetic rat RGMa–specific peptide and affinity purified. As shown in Fig. S2 A (available at http://www.jcb.org/cgi/content/full/jcb.200508143/DC1),

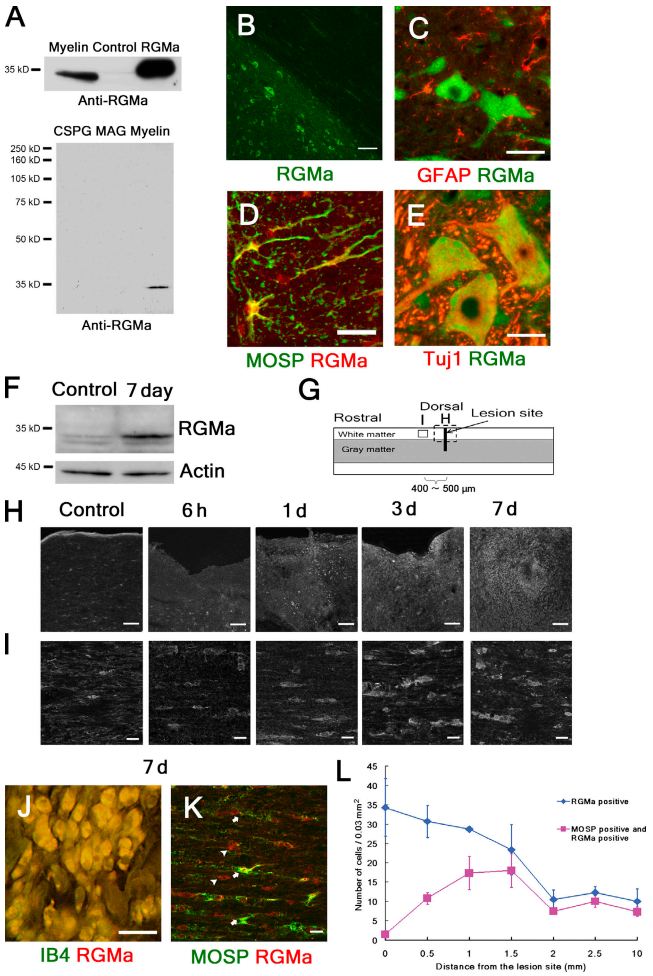

Figure 2. **The expression of RGMa is induced in response to SCI.** (A) Western blot showing the expression of RGMa in purified CNS myelin. (top) Purified myelin and the lysates from control/RGMa CHO cells were blotted with the anti-RGMa antibody. (bottom) CSPG, purified MAG-Fc, and purified myelin were blotted with the anti-RGMa antibody. (B–E) RGMa is expressed in oligodendrocytes and neurons in the rat spinal cord. Fresh frozen tissues were obtained for immunohistochemistry from an uninjured adult rat spinal cord. Parasagittal sections were stained with anti-RGMa (B) or double stained with anti-GFAP and anti-RGMa (C), anti-MOSP and anti-RGMa (D), or anti-Tuj1 and anti-RGMa (E). (C) Double labeling with GFAP and RGMa antibodies shows no colocalization. (D) Double staining with the anti-MOSP and anti-RGMa antibody demonstrates that RGMa is expressed in oligodendrocytes. (E) RGMa immunoreactivity was localized to the somata of Tuj1-positive neurons in the gray matter but not to their axons. (F–L) Western blot analysis and immunohistochemistry reveal upregulated expression of RGMa after SCI. (F) Western blot demonstrates that expression of RGMa is enhanced in the spinal cord tissue 7 d after injury. The protein was detected by an anti-RGMa or anti-actin antibody. An uninjured animal served as the control. (G) Injured spinal cord is illustrated schematically. A dorsal hemisection was performed at Th9/10. Parasagittal fresh frozen sections of an uninjured control spinal cord and those at various postoperative intervals were obtained and used for a time-course study of the immunoreactivity to RGMa in the epicenter area (H) and in the white matter, 400–500 μm rostral to the epicenter area (I). (J) Double staining of the same area as H with IB4 and anti-RGMa reveals the presence of RGMa-expressing microglia/macrophages. (K) Double staining of the same area as I with anti-MOSP and anti-RGMa reveals the presence of double-labeled cells (arrows) and non–double-labeled cells (RGMa-positive and MOSP-negative cells; arrowheads). (L) Quantification of the number of the cells expressing RGMa and those coexpressing RGMa and MOSP. The expression was examined 7 d after SCI. The x axis indicates specific locations along the rostrocaudal axis of the spinal cord. Data are represented as the mean ± SEM of four animals. Bars: (B and H) 100 μm; (C–E and I–K) 20 μm.

the anti-HA antibody as well as the anti-RGMa antibody recognized a protein with an approximate molecular mass of 33 kD in the lysates from the CHO cells expressing HA-tagged RGMa (RGMa-CHO cells). Identical patterns of immunostaining were observed with the anti-HA and anti-RGMa antibody in the RGMa-CHO cells. The anti-RGMa antibody detected a 33-kD band in the purified CNS myelin (Fig. 2 A) and lysates of the rat spinal cord (Fig. 2 F). In addition, we confirmed that the anti-RGMa antibody does not cross-react with chondroitin sulfate proteoglycans (CSPGs) or MAG (Fig. 2 A). The specificity of the antibody was further confirmed by its depleted immunoreactivity with excess antigen peptide (residues 309–322 of rat RGMa) in the injured and noninjured adult spinal cords (Fig. S2 B).

We then performed immunohistochemistry to investigate the distribution pattern of RGMa protein in the adult rat spinal cord. RGMa expression was found in both white and gray matter (Fig. 2 B). Double staining using anti-RGMa and anti–myelin/oligodendrocyte-specific protein (MOSP) antibodies (Dyer et al., 1991; Beck et al., 1995) showed that RGMa was expressed in oligodendrocyte cell bodies and their processes in the white matter (Fig. 2 D). In addition, RGMa was localized to the somata of neuron-specific β tubulin III protein (Tuj1)–positive neurons in the gray matter but not to the axons of these cells (Fig. 2 E). Double immunostaining with the anti-RGMa antibody and the antibody against the glial fibrillary acidic protein (GFAP), an astrocyte marker, showed no colocalization, demonstrating that RGMa is not present in astrocytes (Fig. 2 C). Collectively, RGMa is expressed by neurons and oligodendrocytes, and its expression pattern in the spinal cord is similar to that of Nogo or OMgp (Hunt et al., 2002).

Expression of RGMa is up-regulated after SCI

As our data demonstrate that RGMa inhibits postnatal CNS neurons in vitro (Fig. 1) and that RGMa is expressed by neurons and oligodendrocytes in the adult spinal cord (Fig. 2, B–E), RGMa may play a role in inhibiting axonal regeneration after CNS injury. To test this hypothesis, we examined RGMa expression after SCI. Western blot analysis revealed an increased RGMa expression in the spinal cord 7 d after injury (Fig. 2 F). We performed immunohistochemistry on fresh frozen sections obtained at 6 h and 1, 3, and 7 d after dorsal hemisection of the thoracic spinal cord in rats. RGMa expression was induced around the injury site after the surgery and was detected in the lesion epicenter (Fig. 2, G and H) and the white matter rostral (Fig. 2, G and I) and caudal (not depicted) to the lesion site. In the epicenter area (Fig. 2 H), the tissue structure appeared normal 6 h after injury. Subsequently, when degenerative changes began to be observed 1–3 d after injury, immunoreactivity for RGMa was found in the cells around the lesion site and in areas of aberrant extracellular matrix. This extracellular immunoreactivity may be attributable to the degeneration of RGMa-expressing cells or to the secretion of RGMa by RGMa-positive cells. In the white matter adjacent to the epicenter area (Fig. 2 I), the number of RGMa-immunopositive cells and the intensity of immunoreactivity remained almost unaltered after 6 h. However, 1–3 d after injury, the number of RGMa-positive cells had progressively increased. At 7 d after injury, there was a significant

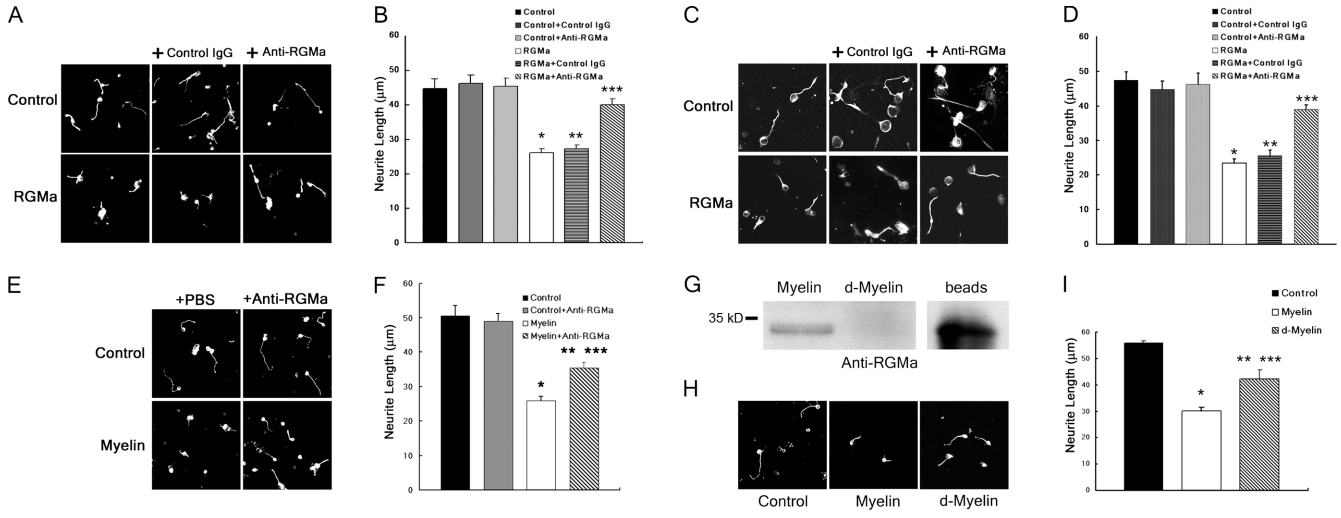

Figure 3. **The anti-RGMa antibody neutralizes the effect of RGMa and CNS myelin in vitro.** (A) The cerebellar neurons were cultured for 24 h on control/RGMa CHO cells in the presence or absence of 10 μg/ml of the control rabbit IgG or anti-RGMa antibody. (B) Mean length of the longest neurite per neuron. *, $P < 0.01$ compared with the control; **, $P < 0.01$ compared with the control + control IgG; ***, $P < 0.01$ compared with RGMa (*t* test). There is no significant difference between the control + anti-RGMa and RGMa + anti-RGMa. (C) Neurons were cultured on PLL-coated chamber slides for 24 h in conditioned media from PI-PLC–treated control CHO/RGMa CHO cells supplemented with or without 10 μg/ml of the control IgG or anti-RGMa antibody. (D) Mean length of the longest neurite per neuron. *, $P < 0.01$ compared with the control; **, $P < 0.01$ compared with the control + control IgG; ***, $P < 0.01$ compared with RGMa (*t* test). There is no significant difference between the control + anti-RGMa and RGMa + anti-RGMa. (E) Neurons were cultured on PLL-coated (control) or PLL + myelin-coated (myelin) chamber slides for 24 h in the presence or absence of 10 μg/ml of the anti-RGMa antibody. (F) Mean length of the longest neurite per neuron. *, $P < 0.01$ compared with the control; **, $P < 0.01$ compared with myelin; ***, $P < 0.01$ compared with the control + anti-RGMa. (G) Immunodepletion of purified CNS myelin. CNS myelin, depleted myelin, and the protein A beads after immunodepletion were blotted with the anti-RGMa antibody. (H) Neurons were cultured on PLL-coated (control), PLL + myelin-coated (myelin), and PLL + depleted myelin-coated (d-Myelin) chamber slides for 24 h. (I) Mean length of the longest neurite per neuron. *, $P < 0.01$ compared with the control; **, $P < 0.03$ compared with myelin; ***, $P < 0.04$ compared with the control. Data are represented as the mean ± SEM of three independent experiments.

increase in the number of RGMa-immunopositive cells in the epicenter area.

We performed a double-labeling experiment 7 d after the injury to characterize the RGMa-expressing cells. Isolectin B4 (IB4)– and RGMa-positive cells were detected in the epicenter area (Fig. 2 J), suggesting that RGMa is expressed in the microglia/macrophages at the lesion epicenter (Streit, 1990). MOSP- and RGMa-positive cells were detected in the white matter adjacent to the epicenter area, demonstrating that RGMa is expressed in the oligodendrocytes in this area. We found that all the MOSP-expressing cells also expressed RGMa, whereas RGMa-positive and MOSP-negative cells were detected particularly around the lesioned site (Fig. 2, K and L). The results of the double staining for IB4 and RGMa suggest that an increase of these cells is attributable to an increase in the number of RGMa-expressing microglia/macrophages in the epicenter area. We did not observe GFAP- and RGMa-positive or Tuj1- and RGMa-positive cells in the lesion epicenter or in the adjacent white matter (unpublished data).

The anti-RGMa antibody neutralizes the inhibitory effect of RGMa and CNS myelin

These results suggest that RGMa with its potent inhibitory activity of neurite outgrowth inhibits axonal regeneration after SCI and that blockage of it offers potential for enhanced recovery after SCI. We therefore investigated whether the anti-RGMa antibody could neutralize the inhibitory activity of RGMa in the coculture assay (Fig. 3, A and B) and the soluble RGMa assay (Fig. 3, C and D). In both assays, the addition of the anti-RGMa antibody but not the control IgG significantly reversed the inhibitory effect of RGMa, demonstrating that the anti-RGMa antibody functions as a neutralizing antibody against RGMa in vitro.

As our data demonstrate that RGMa is expressed by the CNS myelin, the anti-RGMa antibody may reverse the inhibitory activity of the CNS myelin on neurite outgrowth. To test this hypothesis, we cultured neurons on poly-L-lysine (PLL)–coated or PLL + myelin-coated chamber slides for 24 h in the presence or absence of the anti-RGMa antibody (Fig. 3, E and F). The inhibitory activity of myelin on neurite outgrowth was partially blocked by the anti-RGMa antibody. We next performed immunodepletion of the CNS myelin with anti-RGMa antibody and cultured neurons on depleted myelin-coated chamber slides for 24 h. Immunodepletion (Fig. 3 G) partially abolished the inhibitory response (Fig. 3, H and I). Thus, myelin-derived inhibitors except RGMa contribute significantly to the inhibitory response of CNS myelin.

RGMa neutralization leads to functional improvement

We then assessed whether endogenous RGMa acts as an inhibitor of axon regeneration in the injured CNS. We transected two thirds of the dorsal region of rat spinal cords at the vertebral level Th9/10 (lesions 1.8 mm in depth). This resulted in the transection of the main as well as the lateral corticospinal tracts (CSTs). The neutralizing antibodies to RGMa or the control rabbit IgGs were delivered via osmotic minipumps with catheters placed intrathecally near the thoracic injury site. There was no significant difference between the lesion depths in the control and treated groups (Fig. 4 A). The locomotor performance of the animals was monitored over a period of 9 wk after injury. The sham-operated rats (Fig. 4 B) achieved full scores according to the Basso-Beattie-Bresnahan locomotor rating scale (BBB; Basso et al., 1995). All the spinally injured rats became almost completely paraplegic on the first day after the injury (Fig. 4 B) and then gradually displayed partial recovery of locomotor behavior as assessed by the BBB scores. There was no difference in the BBB scores of the anti-RGMa antibody– and control antibody–treated rats up to 4 wk after SCI. In fact, the locomotor performance from 6–9 wk after the surgery was significantly better in rats treated with the anti-RGMa antibody than in those treated with the control antibody. On average, rats treated with the control antibody attained a BBB score of 10.6, whereas those treated with the anti-RGMa antibody achieved a BBB score of 14.9 at 9 wk after the surgery. Thus, the anti-RGMa antibody is effective in treating rats with SCI.

RGMa inhibition induces long-distance growth of injured fiber tracts

The integrity of the dorsal CST in some previously tested rats was assessed by injecting biotin-dextran amine (BDA) into the bilateral sensory-motor cortices. For a group of animals (eight control and six anti-RGMa antibody–treated rats), blocks extending 5 mm rostral and 5 mm caudal to the center of the injury were sectioned in the sagittal plane (Figs. 5 and 6). The far rostral as well as the far caudal segments were sectioned in the transverse plane (Fig. 7). For another group (three control and

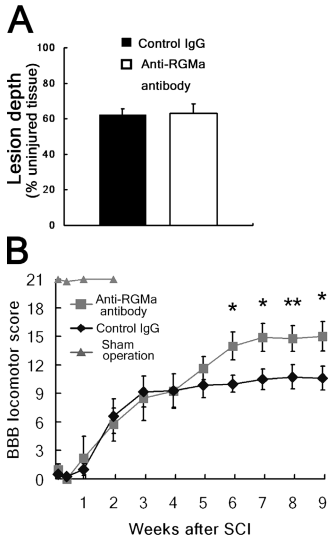

Figure 4. **The anti-RGMa antibody promotes locomotor recovery after SCI.** (A) Quantification of the lesion depth revealed that there was no statistically significant difference between the control and anti-RGMa antibody–treated animals. The significance was determined by *t* test. Mean ± SEM of nine anti-RGMa antibody–treated and 11 control rats. (B) The BBB score was determined at the indicated times after thoracic dorsal hemisection in the anti-RGMa antibody–treated, control antibody–treated, and sham-operated rats. Mean ± SEM of 9, 11, and 5 rats for each group, respectively. The anti-RGMa antibody–treated group is statistically different from the control group, as indicated. *, $P < 0.05$ compared with the control; **, $P < 0.06$ compared with the control.

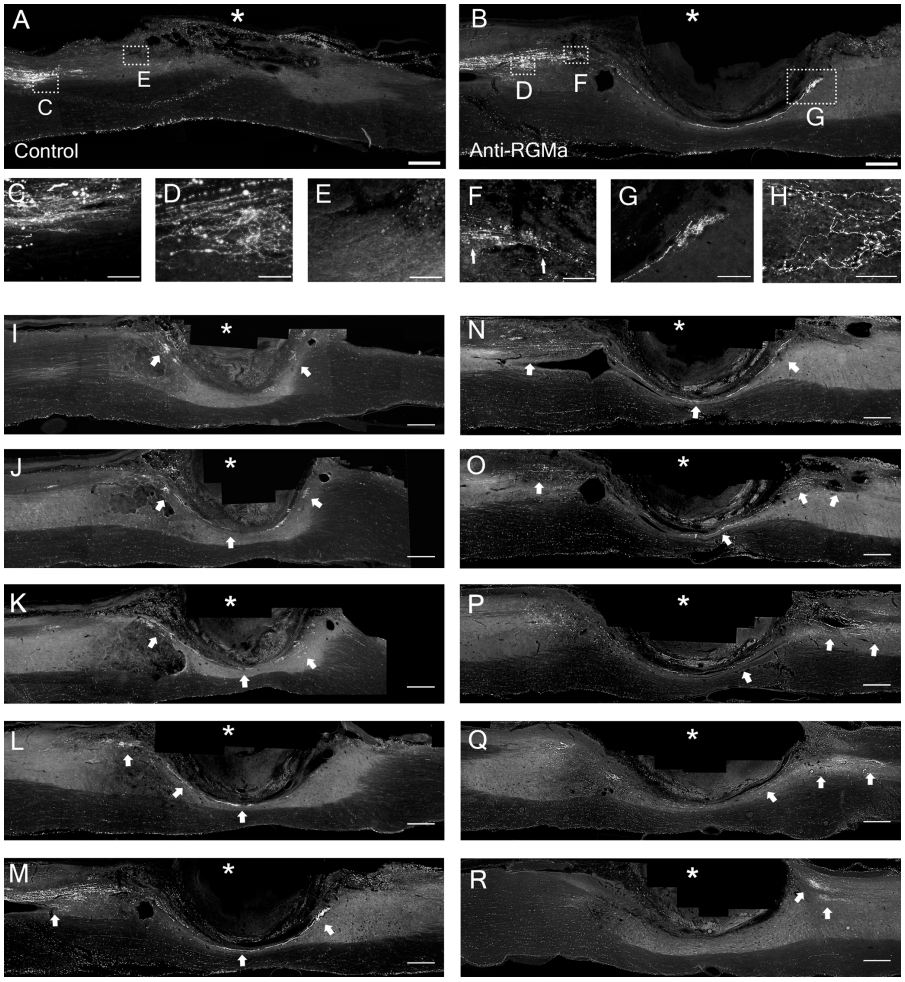

Figure 5. **The anti-RGMa antibody promotes the regeneration/sprouting of CST axons after SCI.** (A and B) Representative pictures of BDA-labeled CST fibers; rostral is on the left. Anterograde-labeled CST fibers in control IgG–treated (A) or anti-RGMa antibody–treated (B) spinal cord 10 wk after injury. The epicenter of the lesion is indicated by an asterisk. (C–G) Higher magnification of the boxed regions in A and B, showing increased collateral CST fiber sprouting rostrally (D), as well as regenerating fibers at the lesion site (F, arrows), in rats treated with the anti-RGMa antibody but not in the corresponding regions of the control IgG–treated rats (C and E). (H) Different sections from the same animal (B), showing regenerating/sprouting fibers in the caudal part of the spinal cord. (I–R) Serial microscopic images of an anti-RGMa antibody–treated animal. Asterisks indicate the epicenter of the lesion. Arrows denote BDA-positive fibers. Bars: (A, B, and I–R) 500 μm; (C–F and H) 100 μm; (G) 200 μm.

three anti-RGMa antibody–treated rats), the spinal cords were sectioned in the transverse plane (Fig. 7).

Samples from the injured rats treated with the anti-RGMa antibody exhibit a completely different pattern of labeling (Fig. 5, B and I–R; and Fig. S5, available at http://www.jcb.org/cgi/content/full/jcb.200508143/DC1), as compared with those from the control antibody–treated rats (Fig. 5 A and Fig. S4, A–J). Proximal to the lesion, the main CST appears as a tight bundle of fibers, with the traced fibers neither entering nor growing beyond the lesion site in the control rats (Fig. 5, A, C, and E). This baseline pattern reflects that axonal regeneration does not normally occur in the CNS. In contrast, numerous ectopic fibers sprouting from the labeled CST were observed both rostral and caudal to the lesion site in rats that were treated with the anti-RGMa antibody (Fig. 5, B and D). The longitudinal sections across the lesion site reveal lower retraction of the main CST bundles and a higher number of collateral CST sprouts in rats treated with the neutralizing antibody (Fig. 5, A and B; and Fig. 6 A). Regenerating fibers with typical irregular meandering growth patterns were frequently observed in the tissue bridges at the level of the lesion in rats treated with anti-RGMa antibody (Figs. 5, D and F; and Fig. S5, A and B). These regenerating fibers extended into the lesion scar, the gray matter caudal to the lesion, and along cysts (Fig. 5, F and H; and Fig. S3). Notably, many axons traversed the lesion tissue, thereby growing either around cavities or within the lesion epicenter, whereas no BDA-traced CST fibers could be detected in the control rats (Fig. 5 E). Bundles of axons extended through the lesion tissue and numerous labeled fibers were observed caudal to the lesion sites in the anti-RGMa antibody–treated rats (Figs. 5, G–K and M–R; and Figs. S3 and S5). In only one rat treated with the anti-RGMa antibody, however, did we not detect BDA-positive fiber in the scar tissue or caudal to the lesion site. Serial microscopic images (Fig. 5, I–R and Fig. S4, A–J) and camera lucida drawings of all the BDA-labeled fibers (Fig. S4, K and L) summarize the pattern of CST fiber growth in the rostral-caudal region of the injury. A few undamaged ventral fibers were illustrated in both cases.

We then reconstructed the serial sections of the injured spinal cords using all the 70–80 serial longitudinal sections per rat and estimated the number of the labeled fibers. In comparison with the number of labeled fibers observed 4 mm rostral to the lesioned site, >20% of the labeled fibers were seen in the caudal spinal cord of rats treated with the anti-RGMa antibody. However, only a small percentage of the fibers (1% at 1 mm caudal to the injury site) were seen in the control antibody–treated rats (Fig. 6 B). Most of these fibers follow branched and tortuous courses, instead of a linear trajectory (Fig. 5 H; Fig. S3, B and C; Fig. S5, B, D, F, and H; and Video 1, available at

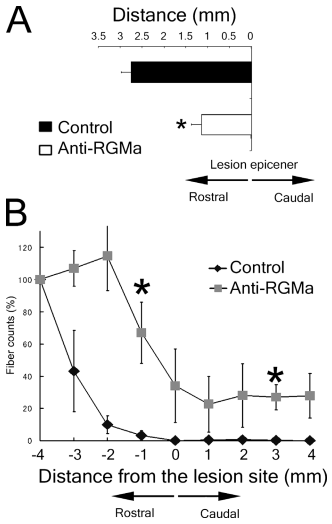

Figure 6. **Quantification of the extent of regeneration/sprouting in anti-RGMa antibody– and control IgG–treated rats.** (A) The distance from the end of the main CST bundles to the lesion epicenter 10 wk after SCI in rats treated with the anti-RGMa antibody or control IgG (n = 6–8 per group). It was measured under low-magnification view of the longitudinal sections. *, $P < 0.01$ compared with the control. The anti-RGMa antibody suppresses the retraction of the injured main CST. (B) Quantification of the labeled CST fibers in six anti-RGMa antibody– and eight control IgG–treated animals. All the 50-μm-thick serial parasagittal sections were evaluated. The x axis indicates specific locations along the rostrocaudal axis of the spinal cord. The y axis indicates the ratio of the number of BDA-labeled fibers at the indicated site to those at 4 mm rostral to the lesion site. *, $P < 0.05$ compared with the control. Error bars indicate SEM.

http://www.jcb.org/cgi/content/full/jcb.200508143/DC1). At the caudal-most part of the regenerating fibers, we observed branches sprouting from the main tract (Fig. 5 G and Fig. S5 F).

We obtained cross-sections of the spinal cord and performed a quantitative analysis of the distribution of the axons to exclude the possibility of axon sparing in the anti-RGMa antibody–treated rats. The total number of labeled fibers 10 mm above the lesion was almost identical between the anti-RGMa and control antibody–treated rats (Fig. 7, A, B, and I), indicating that the extent of BDA uptake was the same between the control and anti-RGMa antibody–treated rats. A thorough serial section reconstruction of the lesion site enabled us to conclude that there was no labeled CST axon that extended past the lesion in the normal locations of the dorsal CST in any of the rats (Fig. 7, C and D). In rats treated with the anti-RGMa antibody, however, BDA-positive fibers with tortuous appearance were detected in the scar tissue developing at the lesion site (Fig. 7, D and E). At 10 mm caudal to the lesion site, the sprouting axons extended through the gray matter to a greater extent than in the white matter in rats treated with the anti-RGMa antibody (Fig. 7, F–H and J–L). Almost no fibers were seen in the ventral part of the dorsal or dorsolateral column in the anti-RGMa antibody–treated rats as well as the control antibody–treated rats (Fig. 7, F and G [insets] and J). The fiber counts in the CST (Fig. 7 J) were not different from those in the negative control (non–BDA-labeled rats; not depicted). There was a little nonspecific staining in the CST, which accounts for the few fiber counts in the CST (Fig. 7 J). These data strongly suggest that there were no spared CST axons, as axons that are spared and extend into the caudal segments should be present in their normal locations. Multiple fibers with tortuous appearance and unusual branching were seen in the gray matter in injured animals treated with the anti-RGMa antibody (Fig. 7, G, H, J, and L). In only one rat treated with the anti-RGMa antibody, however, did we not detect BDA-positive fiber at 1 mm caudal to the injury site. It should be noted that the labeling of the gray matter caudal to the lesion site might be due to sprouting from undamaged ventral fibers. It is not possible to definitely determine long-tract regeneration. Our findings, however, met many of the criteria for identifying regenerated axons (Steward et al., 2003) and raise the possibility that anti-RGMa antibody treatment promotes regrowth of injured CST axons.

Finally, we assessed whether the functional improvement is temporally correlated with the anatomical regeneration. We took consecutive sagittal sections of the spinal cords from anti-RGMa antibody–treated animals 3 and 5 wk after injury (n = 3 for each group). Fig. 8 shows representative pictures of BDA-labeled CST fibers in the control (Fig. 8, A and C) and anti-RGMa antibody–treated animals (Fig. 8, B and D) 5 wk after injury. In anti-RGMa antibody–treated animals, the regenerating fibers extended into the lesion scar but did not extend into the caudal part of the spinal cord (Fig. 8, B and D). In the control rats, there was no labeled CST axon that extended past the lesion (Fig. 8, A and C). We reconstructed the injured spinal cords and assessed the number of the labeled fibers (Fig. 8 E). 3 wk after injury, there was no significant difference between the fiber counts at any distance from the lesion site in anti-RGMa antibody– and control IgG–treated rats (Fig. 8 E). 5 wk after injury, a significant number of BDA-positive fibers (~25% as compared with the number observed 4 mm rostral to the lesioned site) were detected at the lesion epicenter in anti-RGM antibody–treated rats, whereas almost no fibers were seen in the control rats. These results suggest that functional improvement is temporally correlated with anatomical regeneration/sprouting in animals treated with anti-RGMa.

Discussion

The failure of axon regeneration in the spinal cord is at least partly attributable to the growth inhibitory properties of the CNS white matter and the scar tissue developing at the lesion site. Several observations in this study established the notion that RGMa inhibits axon regeneration after SCI. RGMa inhibits neurite outgrowth by activating the RhoA–Rho kinase signaling pathway in vitro and is expressed by oligodendrocytes, myelin, and neurons in the adult rat CNS. After SCI, RGMa expression is induced in the oligodendrocytes and microglia/macrophages around the injury site. The anti-RGMa antibody, which blocks the inhibitory effect of RGMa and CNS myelin in vitro, enhances axonal regeneration/sprouting as well as functional recovery in vivo.

RhoA/Rho kinase and axon growth inhibition

Our data demonstrated that the inhibitory effect of RGM on the neurons is independent of the NgR and is mediated by the RhoA–Rho kinase signaling pathway. This pathway is activated by three

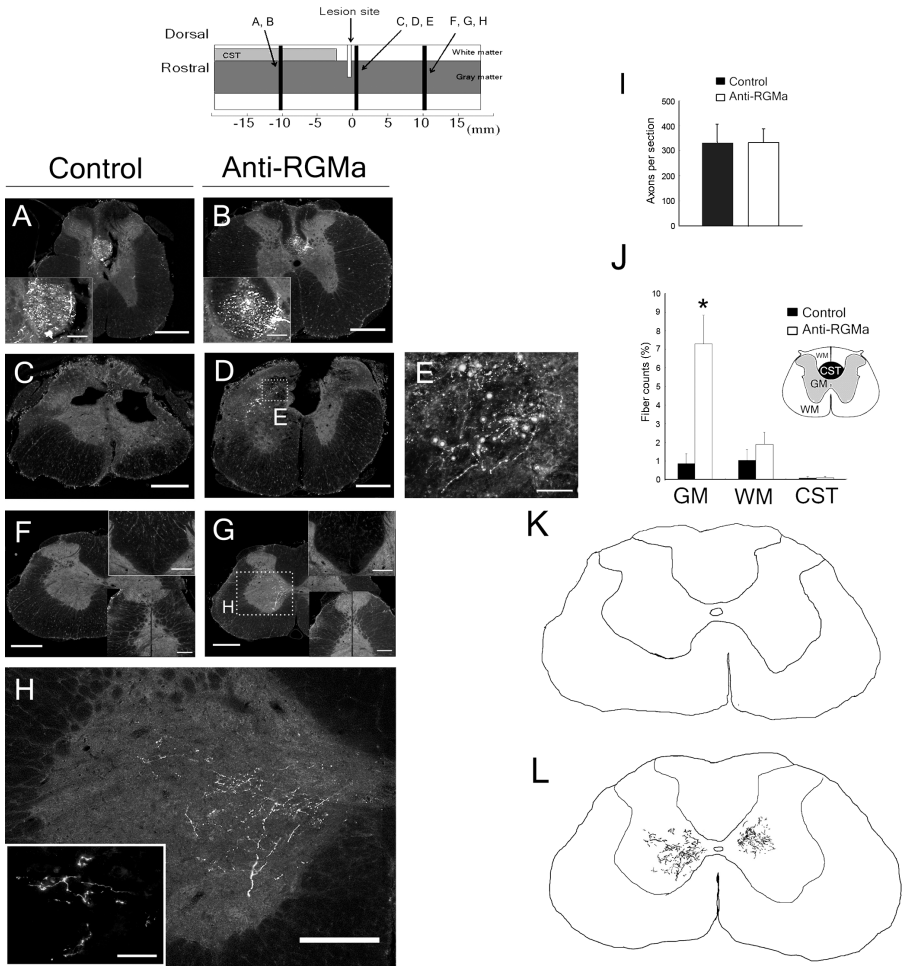

Figure 7. **Distribution of the regenerating/sprouting CST fibers in the spinal cord.** (top) The injured spinal cord is illustrated schematically. (A–H) Representative transverse sections of the spinal cord taken from 10 mm rostral (A and B), 10 mm caudal (F–H), or adjacent (C–E) to the lesioned site from control IgG–treated (A, C, and F) and anti-RGMa antibody–treated (B, D, E, G, and H) rats. Insets of A and B show the high-magnification view of the dorsal CST. (E) High-magnification view in D shows fibers in the developing scar tissue at the lesion site. Insets of F and G illustrate that no fibers are seen in the ventral part of the dorsal column (top right) or dorsolateral column (bottom right) 10 mm caudal to the lesion site. (H) High-magnification view in G shows increased regenerated fibers with tortuous appearance and unusual branching in the gray matter (inset) 10 mm caudal to the lesion site in rats treated with the anti-RGMa antibody. No labeled fibers are observed 10 mm caudal to the lesion site in the corresponding region of the control IgG-treated rats (F). (I) The number of labeled corticospinal axons 10 mm rostral to the lesioned site in rats treated with the control IgG or anti-RGMa antibody. No significant difference is observed. (J) The number of labeled corticospinal axons 10 mm caudal to the lesioned site in rats treated with the control IgG or anti-RGMa antibody. Cross-sections of the spinal cord taken from 10 mm caudal to the lesioned site were examined, and the number of the labeled fibers was estimated in the gray matter (GM), the normal locations of the dorsal CST (CST), or the white matter other than the normal locations of the dorsal CST (WM). Data based on 11 control and 9 anti-RGMa antibody–treated rats. Increase in the regenerating fibers caudal to the lesioned site in the anti-RGMa antibody–treated rats is seen mainly in the gray matter. A small amount of nonspecific staining accounts for a few fiber counts in the CST (no apparent BDA-positive fibers were detected in this area). *, $P < 0.01$ compared with the control. (K and L) Camera lucida drawings illustrating the distribution of BDA-labeled fibers in 10 serial sections from the cases illustrated in F and G, respectively. Bars: (A–D, F, and G) 500 μm; (A, B, F, and G, insets) 200 μm; (E) 50 μm; (H) 200 μm; (H, inset) 50 μm.

well-characterized myelin-associated inhibitors, Nogo, MAG, and OMgp, as well as CSPG, which are expressed both in the glial scar and in myelin (Mueller et al., 2005). Current evidence indicates that a common crucial signaling event for these myelin-derived inhibitors of axon growth is the activation of RhoA. P75 transduces the signal of the three myelin-derived inhibitors of axon regeneration by acting as a displacement factor that releases RhoA from Rho guanine dissociation inhibitor (Yamashita and Tohyama, 2003), which functions to maintain RhoA in an inactive state by sequestering it in the cytoplasm and inhibiting the formation of active RhoGTP. Importantly, Dubreuil et al. (2003) demonstrated that SCI induces RhoA activation in both glial cells and neurons in vivo. They also found that immediate RhoA activation after SCI is p75 dependent but, thereafter, RhoA could be activated in a p75-independent manner. These observations suggest the presence of other molecules that activate RhoA; this is consistent with our findings that RGMa activates RhoA and that its expression is induced around the injury site.

Expression of RGMa in the CNS

An immunohistochemical study of the normal spinal cord shows that RGMa is expressed by neurons and oligodendrocytes. This expression pattern in the spinal cord is similar to that of Nogo or OMgp (Hunt et al., 2002). In the injured spinal cord, however, the expression of RGMa around the lesion site is up-regulated; RGMa is expressed in the microglia/macrophages and oligodendrocytes at the injury site. Our recent report demonstrates that, after SCI, RGMa is expressed by neurons, ballooned neurite fibers/retraction bulbs, oligodendrocytes, smooth muscle/endothelial cells, microglia/macrophages, leucocytes infiltrating the lesion, and with maturation of the lesion, cellular components (e.g., fibroblastoid cells) and extracellular components of the developing scar tissue (cicatrix; Schwab et al., 2005a). In the human brain, a massive up-regulation of RGMa was observed at the lesioned or damaged site after focal cerebral ischemia or traumatic brain injury; RGMa was also present in the scar tissue (Schwab et al., 2005b). These observations suggest the important role of RGMa as an inhibitor of axon regeneration in the injured adult mammalian CNS.

Functional recovery and axon regeneration after SCI

We observed an enhanced locomotor recovery by treatment with the anti-RGMa antibody after SCI. A delayed improvement

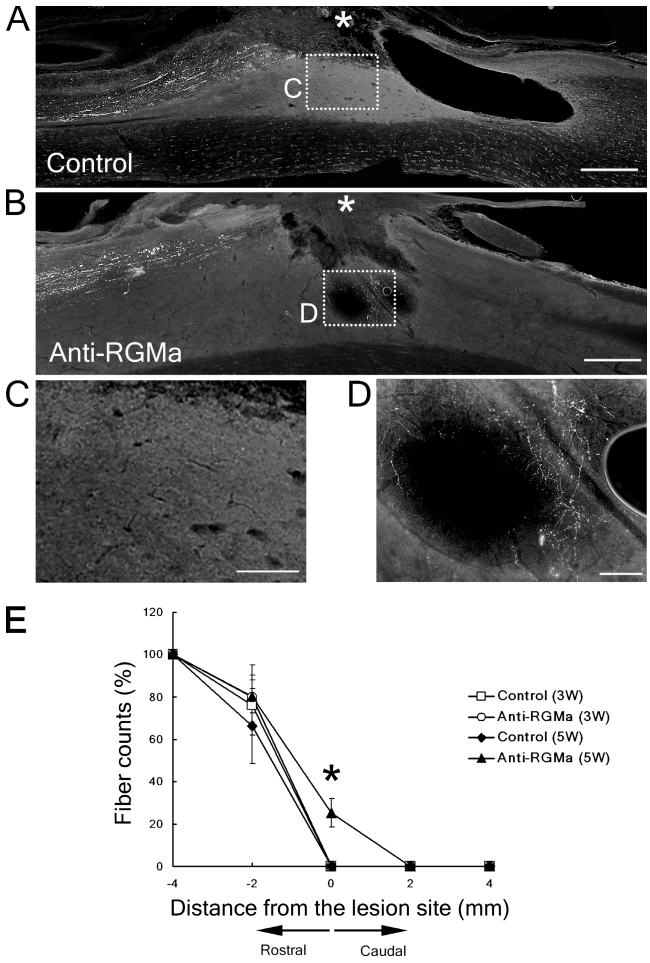

Figure 8. **Anatomical analysis of the spinal cords 3 and 5 wk after SCI.** (A and B) Representative pictures of anterograde-labeled CST fibers in rat spinal cord treated with the control IgG (A) or anti-RGMa antibody (B) 5 wk after injury; rostral is on the left. Asterisks indicate the lesion epicenter. Higher magnification of the boxed regions in A and B, showing regenerating fibers, with typical irregular meandering growth patterns around the cysts at the lesion site (D) in rats treated with the anti-RGMa antibody but not in the corresponding regions of the control IgG–treated rats (C). In both the groups, no BDA-traced fibers could be observed in the caudal part of the spinal cord 5 wk after injury. (E) Quantification of the labeled CST fibers in the anti-RGMa antibody–treated animals 3 wk ($n = 3$) and 5 wk ($n = 3$) after injury and in the control IgG–treated animals 3 wk ($n = 3$) and 5 wk ($n = 3$) after injury. All the 50-μm-thick serial parasagittal sections were evaluated. The x axis indicates specific locations along the rostrocaudal axis of the spinal cord. The y axis indicates the ratio of the number of BDA-labeled fibers at the indicated site to those at 4 mm rostral to the lesion site. *, $P < 0.05$ compared with the control (5W). Bars: (A and B) 500 μm; (C and D) 100 μm.

in locomotor recovery in the anti-RGMa antibody–treated rats might be related to the time course of RGMa expression, which was up-regulated after SCI.

We observed massive fiber growth by anti-RGMa antibody treatment in vivo, whereas the injured axons exhibited little, if any, sprouting in the spinal cord without the treatment. To exclude the possibility that the labeled fibers seen in the caudal portion of the spinal cord are spared axons, we performed thorough reconstructions of the lesioned spinal cord by taking cross-sections (Fig. 7). Multiple fibers with tortuous appearance and unusual branching patterns extended through the gray matter to a greater extent than in the white matter in the caudal portion of the spinal cords of rats treated with the anti-RGMa antibody. The labeled fibers in the gray matter 10 mm caudal to the lesion site are not collaterals of the dorsal CST, as most of the gray matter collaterals of the CST extend in the transverse plane and do not extend for long distances longitudinally through the gray matter (Steward et al., 2003). In fact, analysis of the serial sections of the lesion site from each rat revealed that there was no labeled CST axon that extended past the lesion in the normal locations of the dorsal CST. These findings strongly support our notion that the anti-RGMa antibody promotes regeneration and/or sprouting of injured CST fibers (Steward et al., 2003). However, it is not possible to definitely determine long-tract regeneration. It is possible that the labeling in the gray matter caudal to the lesion site might be due to the sprouting from the undamaged ventral fibers. Evidence suggests that the ventral CST axons collaterally sprout into the gray matter after injury to the dorsal CST (Weidner et al., 2001). Treatment with a high dose of the Rho kinase inhibitor (Y29632), which enhanced functional recovery, induced an increase in the CST profiles in the gray matter distal to the site of injury; this is indicative of collateral sprouting from the ventral spared CST axons (Chan et al., 2005). It is possible to induce the local reorganization of the central pattern generator circuitry, including sprouting from the undamaged ventral fibers, followed by enhanced functional recovery after SCI in anti-RGMa–treated animals.

Mutant mice lacking RGMa may also be useful in determining whether deletion of *RGMa* enhances the regeneration ability. However, as ~50% of the mRGMa mutant mice show defects in cephalic neural tube closure (Niederkofler et al., 2004), conditional knockout mice would be needed to address this issue without considering the effect of RGMa in embryonic development.

Although there is some controversy concerning experiments with targeted gene disruption of the myelin-associated inhibitors, treatments with some neutralizing agents have shown efficacy in promoting regeneration in animal SCI. Similar to our findings in anti-RGMa antibody treatment, treatment with the anti–Nogo A antibody induces regeneration after rat SCI (Bregman et al., 1995). A peptide antagonist, NEP1-40, which competes for binding of Nogo-66 to the NgR, has also shown significant efficacy in terms of promoting regeneration in SCI models (GrandPre et al., 2002; Teng and Tang, 2005). Thus, neutralizing agents including the anti-RGMa antibody may have the potential for clinical applications against SCI (Teng and Tang, 2005).

Signaling mechanism of RGMa

Neogenin is a high-affinity receptor for RGM, mediating its repulsive activity for retinal axons (Rajagopalan et al., 2004). It was recently reported that RGMa mediates BMP signaling by acting as a coreceptor via Smad 1, 5, and 8 and up-regulates the endogenous inhibitor of differentiation (Id1) protein (Babitt et al., 2005). An interaction of RGMa with neogenin along with BMP type I receptor or as a homophilic interaction by itself, as reported for RGMb (dragon; Samad et al., 2004), might underlie its inhibitory activity toward the regeneration of CST fibers.

A clarification of the precise signaling cascade of the RGMa is expected to contribute to the development of more effective therapies for the treatment of adult mammalian CNS injuries.

In summary, our results demonstrate that RGMa is an important inhibitory molecule for successful neuroregeneration in vivo and suggest that its manipulation would be useful for the treatment of human spinal injuries.

Materials and methods

Plasmid constructs
Because the previous report (Monnier et al., 2002) has shown that native chick and functionally active RGM starts with residue 152, we created an HA-RGMa vector in pSecTag2-Hygro (Invitrogen) using the signal peptide of pSecTag2 fused to HA and residues 152–431 of rat RGMa (available from GenBank/EMBL/DDBJ, under accession no. XP_218791). FPC-1-MAG-Fc– and MAG-Fc–expressing CHO cells are gifts from M. Endo and K. Mizuno (Tohoku University, Sendai, Japan).

Generation of RGMa-CHO cells
Flp-in system (Invitrogen) was used to generate RGMa-expressing cells according to the manufacturer's recommendations. We generated an HA-RGMa fragment containing a signal peptide from pSecTag2 vector using two restriction endonucleases and ligated it into pcDNA5FRT (Invitrogen). This construct (pcDNA5FRT/Igκleader/HA/RGMa) and pOG44 were co-transfected into Flp-in CHO cells, and stable expressing cells were generated after growth in medium containing 500 μg/ml Hygromycin B (Invitrogen) for 2 wk. Expression of HA-RGMa was confirmed by immunodetection using Western blots and immunocytochemistry. We also generated human RGMa–expressing cells and confirmed that human RGMa, either membrane bound or diffusible, potently inhibits the neurite outgrowth of postnatal cerebellar granule neurons.

Neurite outgrowth assay
Cerebellar granule cells from rat pups at postnatal days 7–9 were dissociated by trypsinization (0.25% trypsin in PBS for 15 min at 37°C) followed by resuspension in serum-containing medium, trituration, and wash with PBS three times. Cultures were grown in a serum-free DME/F12 medium. For the coculture assay, neurons were plated on confluent monolayers of either RGMa-CHO or control CHO cells in chamber slides (LabTek II; Nunc). For the soluble RGMa assay, confluent monolayers of either RGMa-CHO or control CHO cells were incubated in serum-free DME/F12 medium with or without 2.5 U/ml PI-PLC (Sigma-Aldrich) at 37°C for 3 h. Those treated CHO cells were subjected to the coculture assay. After centrifugation of the culture media at 13,000 *g* for 10 min, the supernatants were collected to remove floating cells. A part of the supernatants was subjected to SDS-PAGE and Western blot analysis to estimate concentration of soluble RGMa with various amounts of the standards (recombinant RGM-A; R&D Systems). Estimated concentration of soluble RGMa was 1.37 (± 0.13 SEM) μg/ml. Neurons were plated in the conditioned media on PLL-coated chamber slides and were incubated for 12 or 24 h. Where indicated, 10 μM of Y27632 (Mitsubishi Pharmaceuticals) was added to the cultures. To inhibit the NgR, 1 μM of NEP(1–40) (Sigma-Aldrich) was added to the culture. For neutralizing antibody assay, anti-RGMa antibody or control rabbit IgG was added to the culture at the concentration of 10 μg/ml. For the neurite outgrowth assay on myelin, we performed myelin preparation from rat brain as described previously (Norton and Padulso, 1973). 3 μg/well of the purified myelin or the depleted myelin were used to coat PLL-coated eight-well chamber slides (Benson et al., 2005). The cells were fixed in 4% (wt/vol) paraformaldehyde and were immunostained with a monoclonal antibody recognizing TuJ1 (1:1,000; Covance). The length of the longest neurite for each β tubulin III–positive neuron was then determined.

Affinity precipitation of GTP-RhoA
Cells were lysed in 50 mM Tris, pH 7.5, 1% Triton X-100, 0.5% sodium deoxycholate, 0.1% SDS, 500 mM NaCl, and 10 mM $MgCl_2$, with leupeptin and aprotinin, each at 10 μg/ml. Cell lysates were clarified by centrifugation at 13,000 *g* at 4°C for 10 min, and the supernatants were incubated with the 20 μg of GST-Rho binding domain of Rhotekin beads (Upstate Biotechnology) at 4°C for 45 min. The beads were washed four times with washing buffer (50 mM Tris, pH 7.5, containing 1% Triton X-100, 150 mM NaCl, 10 mM $MgCl_2$, and 10 μg/ml each of leupeptin and aprotinin). Bound Rho proteins were detected by Western blotting using a monoclonal antibody against RhoA (Santa Cruz Biotechnology, Inc.).

Immunodepletion of RGMa
To examine the remaining effect of myelin-derived inhibitors except RGMa on neurite outgrowth, we subjected the sample to four rounds of immunodepletion (McKerracher et al., 1994). The purified myelin was extracted with 20% octylglucoside salt (Dojindo). The extract was centrifuged at 40,000 *g* for 60 min, and the supernatant was incubated with the 20 μg of anti-RGMa antibody overnight at 4°C. 50 μg of protein A beads were added for 3 h with rotation and centrifuged, and the supernatant was subjected to three repeat treatments. The final depleted samples and the protein A beads were subjected to SDS-PAGE and Western blot analysis, and bioassays were performed as described (see Neurite outgrowth assay).

Western blot analysis
CHO cells, cerebellar granule neurons, or adult rat spinal cords were lysed in 50 mM Tris-HCl, pH 7.5, 150 mM NaCl, 10% glycerol, and 0.5% Brij-58 (Sigma-Aldrich), including protease inhibitor cocktail tablets (Roche Diagnostics). The lysates were clarified by centrifugation at 13,000 *g* at 4°C for 10 min, and the supernatants were collected and normalized for protein concentration. Equal amounts of protein were then boiled in sample buffer containing 12% β-mercaptoethanol for 5 min and subjected to SDS-PAGE. The conditioned media, purified myelin, MAG-Fc, and CSPG (Chemicon) were also treated in the same manner except for the lysis buffer treatment. MAG-Fc was purified from stable expressing cells (provided by K. Mizuno). The proteins were transferred onto polyvinylidene difluoride membrane and incubated with 1 μg/ml of a polyclonal anti-RGMa antibody, a monoclonal anti-HA antibody (1:1,000; Sigma-Aldrich), a polyclonal anti-neogenin antibody (1:1,000; Santa Cruz Biotechnology, Inc.), or a polyclonal anti-actin antibody (1:1,000; Santa Cruz Biotechnology, Inc.). For detection, an ECL chemiluminescence system (GE Healthcare) and HRP-conjugated secondary antibodies (1:1,000; Cell Signaling Technology) were used.

Anti–rat RGMa antibody production
The domain important for functional activity in chick RGM is the COOH-terminal 150–200 amino acids of the active RGM protein. A synthetic peptide (residues 309–322) was selected as immunogen to generate anti–rat RGMa rabbit antisera. The sequence of the peptide is specific to rat RGMa but has no similarity with RGMb or -c. Antisera were affinity purified and used at 1 μg/ml for immunohistochemistry and immunoblots and at 10 μg/ml for neutralizing antibody assay. To assess the specificity of the anti-RGMa antibody, control and SCI sections were stained in the presence of the rat RGMa–specific peptide (residues 309–322; Fig. S2). An additional control experiment was done by leaving out the primary antibody. These experiments confirmed the specificity of the anti-RGMa antibody.

Surgical procedure
Anesthetized (sodium pentobarbital, 40 mg/kg) female Wistar rats (200–250 g) received a laminectomy at vertebral level T9/10, and the spinal cord was exposed. A number 11 blade was used to cut the dorsal part of the spinal cord at a depth of 1.8 mm. Histologic examination has revealed that these lesions sever all dorsal CST fibers in the dorsal funiculus as well as the lateral CST and extend past the central canal in all animals. For neutralizing antibody assay in animal model, immediately after the spinal cord hemisection, rats were fitted with an osmotic minipump (200 μl solution, 0.5 μl/h, 14-d delivery; Alzet pump model 2002 [Durect Co.]) filled with control rabbit IgG (17 animals, 22.3 μg/kg/day over 2 wk; Sigma-Aldrich) or anti-RGMa antibody (15 animals, 22.3 μg/kg/day over 2 wk). The minipump was placed under the skin on the animal's back, and a silastic tube connected to the outlet of the minipump was placed under the dura at the spinal cord hemisection site with the tip lying immediately rostral to the injury site. The tube was sutured to the spinous process just caudal to the laminectomy to anchor it in place. Afterward, the muscle and skin layers were sutured. The bladder was expressed by manual abdominal pressure at least twice a day until bladder function was restored. Sham-operated rats (five animals) received a laminectomy at vertebral level T9/10, and the spinal cords were exposed. The muscle and skin layers were then sutured.

Tissue preparation and immunohistochemistry
For immunohistochemistry, fresh frozen tissues were obtained from an uninjured spinal cord and from ones at 6 h and 1, 3, and 7 d after injury.

After deep anesthesia with diethyl ether, the rats were decapitated and the spinal cords dissected out, embedded in Tissue Tek OCT, and immediately frozen on dry ice at −80°C. Series of parasagittal sections as well as cross-sections were cut at 18 or 50 μm on a cryostat and mounted on APS coating Superfrost-Plus slides (Matsunami). The sections were fixed in 4% (wt/vol) paraformaldehyde for 1 h at room temperature, washed three times with PBS, and blocked in PBS containing 5% goat serum and 0.1% Triton X-100 for 1 h at room temperature. The sections were incubated with primary antibodies overnight at 4°C and washed three times with PBS, followed by incubation with fluorescein-conjugated secondary antibodies (1:1,000; Invitrogen) for 1 h at room temperature. 1 μg/ml of polyclonal anti-RGMa antibody, monoclonal anti-GFAP (1:1,000; Sigma-Aldrich), monoclonal anti-MOSP (1:500; Chemicon), or monoclonal antibody recognizing TuJ1 (1:1,000; Covance) was used as the primary antibody. For double labeling of IB4 from *Griffonia simplicifolia* (1:100; Vector Laboratories) and RGMa, the animals were killed by perfusion with PBS followed by 4% paraformaldehyde. The spinal cords were dissected, postfixed, and heated. Samples were examined under a confocal laser-scanning microscope (Carl Zeiss MicroImaging, Inc.) with 4×, 10×, 20×, 40×, and 63× objectives.

Anterograde labeling of the CST

1 wk (three control and three anti-RGMa antibody–treated rats), 3 wk (three control and three anti-RGMa antibody–treated rats), or 8 wk (11 control and 9 anti-RGMa antibody–treated rats) after injury, descending CST fibers were labeled with BDA (10% in saline, 3.5 μl per cortex, MW 10,000; Invitrogen) injected under anesthesia at the left and the right motor cortices (coordinates: 2 mm posterior to bregma, 2 mm lateral to bregma, 1.5 mm depth). For each injection, 0.25 μl of BDA was delivered for a period of 30 s via a 15–20-μm inner diameter glass capillary attached to a microliter syringe (ITO). In total, we examined and compared the regenerative responses of 17 control and 15 anti-RGMa antibody–treated rats after SCI. 14 d after BDA injection, the animals were killed by perfusion with PBS followed by 4% paraformaldehyde. The spinal cords were dissected, postfixed overnight in the same fixatives, and cryopreserved in 30% sucrose in PBS. The spinal cord 5 mm rostral and 5 mm caudal to the lesion site (10 mm long) was embedded in Tissue Tek OCT. These blocks were sectioned in the sagittal plane (50 μm) or in the transverse plane, retaining each section. In both cases, transverse sections were also collected from the spinal cord >5 mm rostral and caudal to the injury site (17 control and 15 anti-RGMa antibody–treated rats). Sections were blocked in PBS with 0.5% BSA for 1 h and then incubated for 1 d with Alexa Fluor 488–conjugated streptavidin (1:400; Invitrogen) in PBS with 0.15% BSA.

Quantification

To reconstruct serial parasagittal sections completely, all serial 50-μm-thick sections (~70–80 sections per animal; eight control and six anti-RGMa antibody–treated rats in Fig. 6 B, six control and six anti-RGMa antibody–treated rats in Fig. 8 E) were evaluated. On each section, the number of intersections of BDA-labeled fibers with a dorsoventral line was counted from 4 mm above to 4 mm below the lesion site. Axon number was calculated as a percentage of the fibers seen 4 mm above the lesion, where the CST was intact. The distance beyond the epicenter of the lesion was scored as positive and otherwise as negative distance.

The distance from the end of the main CST bundles to the lesion epicenter was measured for each animal for quantification of the retraction of CST fibers. The distance beyond the epicenter of the lesion was scored as positive and otherwise as negative distance.

To exclude the possibility of axon sparing in the anti-RGMa antibody–treated rats, we took thorough serial cross-sections of the spinal cord and performed quantitative analysis of the distribution of the axons (11 control and 9 anti-RGMa antibody–treated rats). Degrees of BDA uptake were assessed by counting the total number of fibers in the cross-section 10 mm rostral to the lesioned site. For quantification of the number of labeled corticospinal axons 10 mm caudal to the lesion site, the number of the labeled fibers was measured for each animal in the gray matter, the dorsal CST area (normal locations of the dorsal CST), or the white matter except the dorsal CST area, divided by the number of labeled corticospinal axons 10 mm above the lesion.

For camera lucida drawing, all consecutive parasagittal sections from 4 mm above to 4 mm below the injury site or transverse sections around 10 mm caudal the lesion site were imaged, and BDA-positive CST axons were traced.

Behavioral testing

Behavioral recovery was assessed for 9 wk after injury in an open field environment by the BBB. Uninjured and sham-operated rats ($n = 5$) achieved full scores. Quantification was performed in a blinded manner by two (the first group; eight control and six anti-RGMa antibody–treated rats) or three (the second group; three control and three anti-RGMa antibody–treated rats) observers. The difference of judged counts among the observers was within 1 point on the BBB scoring scale.

Online supplemental material

Fig. S1 demonstrates that cerebellar granule neurons express neogenin. Fig. S2 shows specificity of the anti-RGMa antibody. Fig. S3 shows regenerated CST axons with the anti-RGMa antibody treatment. Fig. S4 displays serial microscopic images of a control IgG–treated rat and reconstruction of the lesioned spinal cords treated with control IgG or the anti-RGMa antibody. Fig. S5 shows injured spinal cords of four animals with anti-RGMa antibody treatment. Video 1 shows regenerated CST axons with the anti-RGMa antibody treatment. Online supplemental material is available at http://www.jcb.org/cgi/content/full/jcb.200508143/DC1.

We thank M. Endo and K. Mizuno for gifts of FPC-1-MAG-Fc– and MAG-Fc–expressing CHO cells.

This work was supported by a research grant from the National Institute of Biomedical Innovation (05-12); Takeda Science Foundation; a grant-in-aid from the Ministry of Education, Culture, Sports, Science and Technology (15390438); and a research grant for nervous and mental disorders from the Ministry of Health, Labour and Welfare (15A-2).

Submitted: 22 August 2005
Accepted: 8 March 2006

References

Babitt, J.L., Y. Zhang, T.A. Samad, Y. Xia, J. Tang, J.A. Campagna, A.L. Schneyer, C.J. Woolf, and H.Y. Lin. 2005. Repulsive guidance molecule (RGMa), a DRAGON homologue, is a bone morphogenetic protein co-receptor. *J. Biol. Chem.* 280:29820–29827.

Basso, D.M., M.S. Beattie, and J.C. Bresnahan. 1995. A sensitive and reliable locomotor rating scale for open field testing in rats. *J. Neurotrauma.* 12:1–21.

Beck, K.D., L. Powell-Braxton, H.R. Widmer, J. Valverde, and F. Hefti. 1995. *Igf1* gene disruption results in reduced brain size, CNS hypomyelination, and loss of hippocampal granule and striatal parvalbumin-containing neurons. *Neuron.* 14:717–730.

Benson, M.D., M.I. Romero, M.E. Lush, Q.R. Lu, M. Henkemeyer, and L.F. Parada. 2005. Ephrin-B3 is a myelin-based inhibitor of neurite outgrowth. *Proc. Natl. Acad. Sci. USA.* 102:10694–10699.

Bregman, B.S., E. Kunkel-Bagden, L. Schnell, H.N. Dai, D. Gao, and M.E. Schwab. 1995. Recovery from spinal cord injury mediated by antibodies to neurite growth inhibitors. *Nature.* 378:498–501.

Chan, C.C., K. Khodarahmi, J. Liu, D. Sutherland, L.W. Oschipok, J.D. Steeves, and W. Tetzlaff. 2005. Dose-dependent beneficial and detrimental effects of ROCK inhibitor Y27632 on axonal sprouting and functional recovery after rat spinal cord injury. *Exp. Neurol.* 196:352–364.

David, S., and A.J. Aguayo. 1981. Axonal elongation into peripheral nervous system "bridges" after central nervous system injury in adult rats. *Science.* 214:931–933.

Dubreuil, C.I., M.J. Winton, and L. McKerracher. 2003. Rho activation patterns after spinal cord injury and the role of activated Rho in apoptosis in the central nervous system. *J. Cell Biol.* 162:233–243.

Dyer, C.A., W.F. Hickey, and E.E. Jr. Geisert. 1991. Myelin/oligodendrocyte-specific protein: a novel surface membrane protein that associates with microtubules. *J. Neurosci. Res.* 28:607–613.

GrandPre, T., S. Li, and S.M. Strittmatter. 2002. Nogo-66 receptor antagonist peptide promotes axonal regeneration. *Nature.* 417:547–551.

Hunt, D., R.S. Coffin, and P.N. Anderson. 2002. The Nogo receptor, its ligands and axonal regeneration in the spinal cord; a review. *J. Neurocytol.* 31:93–120.

Manitt, C., K.M. Thompson, and T.E. Kennedy. 2004. Developmental shift in expression of netrin receptors in the rat spinal cord: predominance of UNC-5 homologues in adulthood. *J. Neurosci. Res.* 77:690–700.

Matsunaga, E., S. Tauszig-Delamasure, P.P. Monnier, B.K. Mueller, S.M. Strittmatter, P. Mehlen, and A. Chedotal. 2004. RGM and its receptor neogenin regulate neuronal survival. *Nat. Cell Biol.* 6:749–755.

McKerracher, L., S. David, D.L. Jackson, V. Kottis, R.J. Dunn, and P.E. Braun. 1994. Identification of myelin-associated glycoprotein as a major myelin-derived inhibitor of neurite growth. *Neuron.* 13:805–811.

Monnier, P.P., A. Sierra, P. Macchi, L. Deitinghoff, J.S. Andersen, M. Mann, M. Flad, M.R. Hornberger, B. Stahl, F. Bonhoeffer, and B.K. Mueller.

2002. RGM is a repulsive guidance molecule for retinal axons. *Nature.* 419:392–395.

Muller, B.K., D.G. Jay, and F. Bonhoeffer. 1996. Chromophore-assisted laser inactivation of a repulsive axonal guidance molecule. *Curr. Biol.* 6:1497–1502.

Mueller, B.K., H. Mack, and N. Teusch. 2005. Rho kinase, a promising drug target for neurological disorders. *Nat. Rev. Drug Discov.* 4:387–398.

Niederkofler, V., R. Salie, M. Sigrist, and S. Arber. 2004. Repulsive guidance molecule (RGM) gene function is required for neural tube closure but not retinal topography in the mouse visual system. *J. Neurosci.* 24:808–818.

Norton, W.T., and S.E. Poduslo. 1973. Myelination in rat brain: method of myelin isolation. *J. Neurochem.* 21:749–757.

Oldekamp, J., N. Kramer, G. Alvarez-Bolado, and T. Skutella. 2004. Expression pattern of the repulsive guidance molecules RGM A, B and C during mouse development. *Gene Expr. Patterns.* 4:283–288.

Rajagopalan, S., L. Deitinghoff, D. Davis, S. Conrad, T. Skutella, A. Chedotal, B.K. Mueller, and S.M. Strittmatter. 2004. Neogenin mediates the action of repulsive guidance molecule. *Nat. Cell Biol.* 6:756–762.

Ren, X.D., W.B. Kiosses, and M.A. Schwartz. 1999. Regulation of the small GTP-binding protein Rho by cell adhesion and the cytoskeleton. *EMBO J.* 18:578–585.

Samad, T.A., A. Srinivasan, L.A. Karchewski, S.J. Jeong, J.A. Campagna, R.R. Ji, D.A. Fabrizio, Y. Zhang, H.Y. Lin, E. Bell, and C.J. Woolf. 2004. DRAGON: a member of the repulsive guidance molecule-related family of neuronal- and muscle-expressed membrane proteins is regulated by DRG11 and has neuronal adhesive properties. *J. Neurosci.* 24:2027–2036.

Schmidtmer, J., and D. Engelkamp. 2004. Isolation and expression pattern of three mouse homologues of chick Rgm. *Gene Expr. Patterns.* 4:105–110.

Schwab, J.M., S. Conrad, P.P. Monnier, S. Julien, B.K. Mueller, and H.J. Schluesener. 2005a. Spinal cord injury-induced lesional expression of the repulsive guidance molecule (RGM). *Eur. J. Neurosci.* 21:1569–1576.

Schwab, J.M., P.P. Monnier, H.J. Schluesener, S. Conrad, R. Beschorner, L. Chen, R. Meyermann, and B.K. Mueller. 2005b. Central nervous system injury-induced repulsive guidance molecule expression in the adult human brain. *Arch. Neurol.* 62:1561–1568.

Stahl, B., B. Muller, Y. von Boxberg, E.C. Cox, and F. Bonhoeffer. 1990. Biochemical characterization of a putative axonal guidance molecule of the chick visual system. *Neuron.* 5:735–743.

Steward, O., B. Zheng, and M. Tessier-Lavigne. 2003. False resurrections: distinguishing regenerated from spared axons in the injured central nervous system. *J. Comp. Neurol.* 459:1–8.

Streit, W.J. 1990. An improved staining method for rat microglial cells using the lectin from *Griffonia simplicifolia* (GSA I-B4). *J. Histochem. Cytochem.* 38:1683–1686.

Teng, F.Y., and B.L. Tang. 2005. Why do Nogo/Nogo-66 receptor gene knockouts result in inferior regeneration compared to treatment with neutralizing agents? *J. Neurochem.* 94:865–874.

Uehata, M., T. Ishizaki, H. Satoh, T. Ono, T. Kawahara, T. Morishita, H. Tamakawa, K. Yamagami, J. Inui, M. Maekawa, and S. Narumiya. 1997. Calcium sensitization of smooth muscle mediated by a Rho-associated protein kinase in hypertension. *Nature.* 389:990–994.

Weidner, N., A. Ner, N. Salimi, and M.H. Tuszynski. 2001. Spontaneous corticospinal axonal plasticity and functional recovery after adult central nervous system injury. *Proc. Natl. Acad. Sci. USA.* 98:3513–3518.

Yamashita, T., and M. Tohyama. 2003. The p75 receptor acts as a displacement factor that releases Rho from Rho-GDI. *Nat. Neurosci.* 6:461–467.